PROCEEDINGS B

royalsocietypublishing.org/journal/rspb

Research

Cite this article: Eskew EA, Clancey E, Singh D, Situma S, Nyakarahuka L, Njenga MK, Nuismer SL. 2026 Interepidemic Rift Valley fever in East Africa: the recent risk landscape and projected impacts of global change. *Proc. R. Soc. B* **293**: 20252193. https://doi.org/10.1098/rspb.2025.2193

Received: 26 August 2025
Accepted: 9 December 2025

Subject Category:
Ecology

Subject Areas:
health and disease and epidemiology, ecology

Keywords:
climate change, emerging infectious disease, force of infection, machine learning, mosquito-borne disease, population growth, serology, shared socioeconomic pathways, vector-borne disease, zoonosis

Author for correspondence:
Evan A. Eskew
e-mail: evane@uidaho.edu

Electronic supplementary material is available online at https://doi.org/10.6084/m9.figshare.c.8230314.

THE ROYAL SOCIETY PUBLISHING

Interepidemic Rift Valley fever in East Africa: the recent risk landscape and projected impacts of global change

Evan A. Eskew[1], Erin Clancey[3], Deepti Singh[4], Silvia Situma[5,6], Luke Nyakarahuka[7,8], M. Kariuki Njenga[3,5] and Scott L. Nuismer[2]

[1]Institute for Interdisciplinary Data Sciences, and [2]Department of Biology, University of Idaho, Moscow, ID, USA
[3]Paul G. Allen School for Global Health, Washington State University, Pullman, WA, USA
[4]School of the Environment, Washington State University, Vancouver, WA, USA
[5]Global Health-Kenya, Washington State University, Nairobi, Kenya
[6]Department of Animal Science, Pwani University, Kilifi, Kenya
[7]Department of Biosecurity, Ecosystems and Veterinary Public Health, Makerere University, Kampala, Uganda
[8]Uganda Virus Research Institute, Entebbe, Uganda

EAE, 0000-0002-1153-5356; EC, 0000-0003-4728-4023; SLN, 0000-0001-9817-0056

Rift Valley fever (RVF) is a zoonotic disease that causes sporadic, multi-country epidemics. However, there is limited understanding of RVF virus circulation during interepidemic periods and the potential impacts of global change on interepidemic RVF. To address these knowledge gaps, we built a predictive model using recent interepidemic RVF outbreak data from Kenya, Tanzania and Uganda. We then projected interepidemic RVF risk for three future time periods (2021–2040, 2041–2060, 2061–2080) under three global change scenarios representing different trajectories for climate and human population distribution (SSP126, SSP245, SSP370). Our model identified interepidemic RVF risk hotspots in east Kenya, east Tanzania and southwest Uganda. Hydrology was a major driver of disease risk: hotspots emerged in association with lakes and rivers, and risk peaked during May–July following the long rains season (March–May). Projections under global change scenarios suggested that disease risk will generally decrease over time. Nevertheless, owing to expected human population growth, we estimate that >90 million people in the study region will be exposed to interepidemic RVF by 2061–2080, which is nearly double the historical (1970–2000) estimate of approximately 49 million people. Mitigating the future health impacts of RVF will require increased disease surveillance, prevention and control effort in risk hotspots.

1. Introduction

Rift Valley fever (RVF), a mosquito-borne zoonotic disease caused by RVF virus (RVFV), affects Africa and the Arabian Peninsula [1]. RVF is a unique threat because, in addition to causing human morbidity and mortality, disease outbreaks can impact the livestock trade that supports hundreds of millions of livelihoods throughout Africa [1,2]. To counteract RVF's devastating health and economic burden, models have been developed to predict when and where major regional epidemics could emerge. RVF outbreaks often occur following excessive rainfall [3,4] when flooding creates aquatic breeding habitats that fuel the growth of RVFV-infected mosquito populations [1,5–7]. Disease forecasts have leveraged this information by using the normalized difference vegetation index (NDVI), a satellite-derived measure of vegetation growth in response to rainfall, to predict impending RVF epidemics [5,7,8]. This near-term forecasting approach enabled prediction of the multi-country

2006–2007 RVF epidemic weeks before it occurred, facilitating early warning of the at-risk human population [9].

Despite the promise of these predictive methods, the traditional research focus on large, but relatively infrequent, regional RVF epidemics is challenged by increased recognition of RVF activity during interepidemic periods [10,11]. For example, RVFV circulates endemically in humans across East Africa, including in Kenya [12–14], Tanzania [15–17] and Uganda [18–21]. Interepidemic RVF, while underappreciated relative to regional epidemics, is of significant public health concern given human morbidities and deaths caused by RVFV infection during interepidemic periods [14,20,21]. Interepidemic RVF may also demand a modified disease prediction paradigm: numerous factors besides rainfall, including elevation, topography, soils and various aspects of human or livestock host populations, plausibly influence interepidemic RVFV dynamics at fine spatial scales [6,12,22–24].

Our predictive understanding of RVF is further complicated by global change processes, particularly climate and human population change, which promise to shift the risk landscape of numerous infectious diseases [25–27]. Climate change can have multifaceted effects on the arthropod vectors of zoonotic diseases, including influences on pathogen transmission efficiency and vector distribution [28]. As such, climate change is expected to alter RVF's spatial extent and magnitude of impact [5,29–31]. Similarly, human population density and anthropogenic environmental pressures associated with urban areas can shape a landscape's suitability for vector-borne disease transmission [32]. Existing methods for RVF forecasting are primarily focused on near-term prediction of regional epidemics (i.e. they focus on early warning, weeks or months ahead of large RVF outbreaks). These approaches do not allow for RVF risk prediction over the longer timescales relevant to global change processes nor do they address disease risk during interepidemic periods [2]. Consequently, we do not yet understand how global change is likely to alter interepidemic RVF risk, and this knowledge gap hinders effective prioritization of research, policy and public health practices (e.g. vaccine allocation) that could ensure healthier futures.

Here we use machine learning to analyse interepidemic RVF outbreak data (figure 1) and to project interepidemic RVF risk under three future global change scenarios across Kenya, Tanzania and Uganda (hereafter, 'the study region'). Our specific objectives were to: (i) model recent interepidemic RVF outbreaks to learn relationships between environmental and biological features and interepidemic RVF risk; (ii) validate the interepidemic RVF risk model using independent IgG serological data from humans; (iii) project interepidemic RVF risk under global change scenarios using learnt relationships from the validated model; and (iv) estimate the human population at risk from interepidemic RVF under global change scenarios. Ultimately, our analyses identify key abiotic and biotic factors that are associated with interepidemic RVF outbreaks, estimate the recent risk landscape for interepidemic RVF across East Africa and project how changing environmental conditions and human population distribution in the coming decades will translate to changes in that risk landscape.

2. Methods

Our analysis workflow had four discrete steps. First, we used a machine learning model to identify the environmental and biological features that predict recent interepidemic RVF outbreaks. Using the model, we were able to retrodict the relative likelihood of interepidemic RVF across the study region for all months from 2008 to 2022. Second, we validated these retrodictions using IgG serological data from humans—data that were never used in model training. Third, we used the validated model to develop projections of interepidemic RVF risk across the study region for three future time periods (2021–2040, 2041–2060, 2061–2080) under three global change scenarios (SSP126, SSP245, SSP370; electronic supplementary material, 'The Shared Socioeconomic Pathways'). These global change scenarios represent potential future trajectories for climate and human population distribution over the coming decades. Finally, we estimated the human population at risk from interepidemic RVF under each future scenario. We describe each analytical step in greater detail below.

(a) Modelling recent interepidemic RVF outbreaks

To train a predictive model of interepidemic RVF, we used spatially and temporally explicit disease presence and absence data, as well as associated predictor variables. Here we describe our procedures for defining RVF presence and absence locations, collating predictor variables and training the machine learning model.

(i) Interepidemic RVF outbreak and background data

To model interepidemic RVF risk, we required disease presence and absence data (i.e. outbreak and background points) from across the study region.

For disease presence data, we updated an existing dataset of livestock and human RVF outbreaks that occurred in 2008 or later, following the large 2006–2007 East African RVF epidemic [31]. Given that all the outbreaks occurred after the 2006–2007 epidemic, we considered them as representative of interepidemic disease transmission. As such, our work investigates the factors that drive RVF cases, but we do not address the large, multi-country epidemics that often dominate discussion in the RVF literature. Interepidemic RVF outbreak events were primarily defined by viral detection via PCR or positive IgM antibody tests, indicative of current or recent RVFV infection, respectively. We also drew on case reports from global health authorities (e.g. the World Organisation for Animal Health).

To ensure our updated outbreak dataset provided comprehensive coverage of interepidemic RVF events during the focal period, we performed a Web of Science search to capture additional relevant literature. We used the following search query string: '('Kenya' OR 'Uganda' OR 'Tanzania') AND ('Rift Valley fever' OR 'RVF') AND ('interepidemic' OR 'inter-epidemic' OR

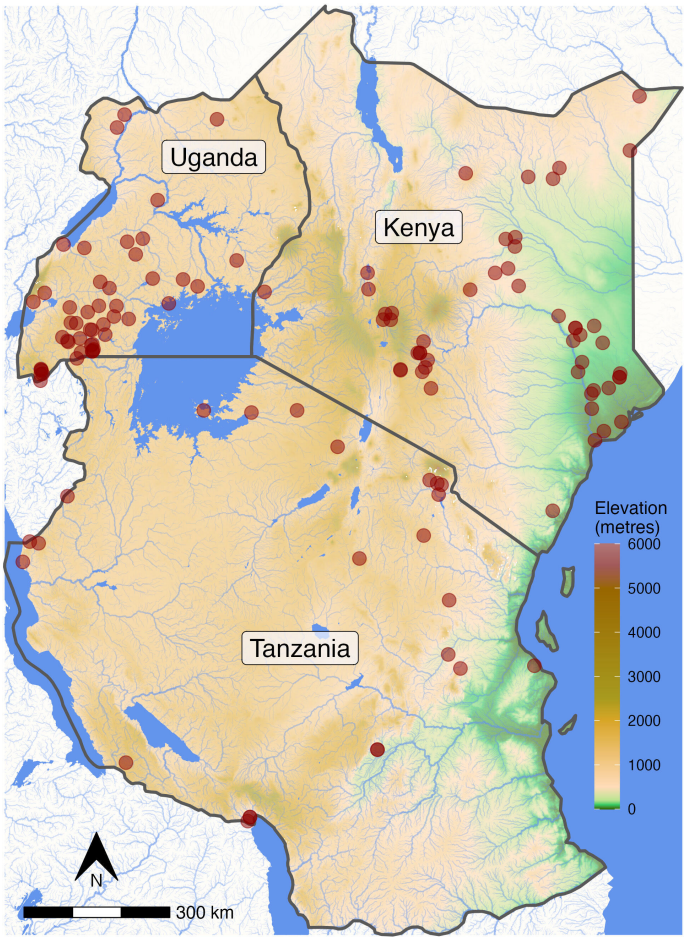

Figure 1. Topographic map of Kenya, Tanzania and Uganda showing the locations (red points) of 122 interepidemic RVF outbreak events from 2008 to 2022. Background colour represents elevation across the study region. Note that a subset of outbreak events ($n = 25$) for which precise locations were unknown are plotted at their administrative unit centroids.

'enzootic' OR 'IgM' OR 'PCR' OR 'qPCR' OR 'cross-sectional' OR 'laboratory-confirmed')'. This search returned 181 papers. We read the abstracts of all 181 papers to identify literature that probably matched our criteria (i.e. studies providing PCR or IgM data for the study region during the focal interepidemic period). We conducted an in-depth review of the 28 papers that passed this filtration step, attempting to extract data. We identified usable data in 22 of these 28 papers, and if not already represented in our outbreak dataset, we incorporated this new information. Our updated outbreak dataset was composed of 122 small RVF outbreaks (< 40 cases each) occurring in Kenya, Tanzania and Uganda from 2008 to 2022 [33] (figure 1).

Wherever possible, RVF outbreak locations were defined using GPS coordinates. However, for 25 of the 122 outbreaks, it was either impossible to precisely define the outbreak location or the data collection context (e.g. health facility sampling) suggested that the sampling location was not the true outbreak location. The location of these 25 outbreaks was defined as narrowly as possible using administrative units. For downstream analyses, we then employed a data replication approach to adequately represent uncertainty in outbreak location [34]. Specifically, we generated 10 duplicate sets of our RVF outbreak data. Outbreak points known to the level of GPS coordinates were assigned their known coordinates in each data replicate. However, outbreak points known only to the level of administrative unit were randomly assigned GPS coordinates within their administrative unit in each data replicate. This data replication procedure generated a dataset of 1220 outbreak points, all with assigned GPS coordinates, which we used for all further analyses.

For disease absence data, we generated a total of 27 000 background points from across the study region, 150 from each month from 2008 to 2022 (electronic supplementary material, figure S1). Critically, to reduce the effects of disease reporting bias in our model, we followed the approach of Gibb *et al.* [35] and generated background points in proportion to human population density (electronic supplementary material, 'Background Data').

(ii) Predictor variables

To train our model, we used a suite of 31 spatially explicit predictors, including variables capturing physical landscape features (e.g. hydrology, soil characteristics, topography), weather (e.g. precipitation, temperature), disease detection capacity (e.g. travel time to healthcare) and the abundance of key RVFV hosts (e.g. human and livestock density) (electronic supplementary material, table S1). These predictors have been implicated in driving RVF risk across spatial scales [4,6,22,24]. We processed all predictor variable rasters to a spatial resolution of 2.5 arcminutes (4.63 km × 4.63 km grid cells at the equator). Given this resolution, the study region was covered by a total of 124 313 grid cells. We operate with this grid cell layout throughout our project workflow. More details on predictor variables can be found in the electronic supplementary material, 'Predictor Variables' section.

(iii) Model training and evaluation

Once interepidemic RVF outbreak points, background points and predictor variables were collated, we fit gradient-boosted decision trees using XGBoost [36]. Prior to model training, we split our collated dataset of outbreak and background points into training and test datasets. Given our interest in developing a machine learning model that could make accurate predictions of future RVF risk, we intentionally split the data such that the model was evaluated using a test dataset that was temporally disjunct from any data used during model training. Training data consisted of all points from 2008 to 2018 (920 RVF outbreak points [after data replication] and 19 800 background points; 1 : 22 class ratio), while the test dataset consisted of all points from 2019 to 2022 (300 RVF outbreak points [after data replication] and 7200 background points; 1 : 24 class ratio). We tuned model hyperparameters using cross-validation and evaluated model performance on the test dataset using the area under the receiver operating characteristic curve (AUC-ROC) measure (electronic supplementary material, 'Model Training'). Our data were imbalanced, a common scenario in presence–background modelling [37], but AUC-ROC is robust to class imbalance [38].

Using the trained model, we generated historical predictions (retrodictions) of the relative likelihood of interepidemic RVF across the study region for all months from 2008 to 2022. To be explicit about our terminology, we follow examples from the species distribution modelling literature and call the predictive output from our model 'relative likelihood' values so that these values are not interpreted as well-calibrated probabilities [37,39]. Furthermore, we take relative likelihood values as a proxy for interepidemic RVF risk and therefore use these terms interchangeably throughout. While the model training process only used predictor data from grid cells containing outbreak or background points, retrodictions used predictor data from across the entire study region (i.e. we made retrodictions for every grid cell). Generating model-based retrodictions from 2008 to 2022 allowed us to investigate recent temporal and spatial patterns in the relative likelihood of interepidemic RVF. We performed all model fitting and analysis in R version 4.4.1 [40] using the *tidymodels* package collection [41].

(b) Independent model validation

We validated our model's predictive ability using IgG serological data, a fully independent data source, to generate estimates of RVFV force of infection (FOI) into the human population. First, we compiled published and unpublished anti-RVFV IgG serological data from humans across the study region [17,42], targeting individual-level data where serostatus, location and age were known. In contrast to the PCR or IgM detections used to define our RVF outbreak dataset, IgG antibodies provide long-lasting signals of prior RVFV exposure. Our data compilation efforts recovered a total of 6557 IgG serological assays (i.e. ELISA tests) across Kenya (n = 5255), Tanzania (n = 542) and Uganda (n = 760), representing 216 seropositive individuals (3.3% seroprevalence). Second, based on geographic location, we assigned each serological assay to its corresponding 2.5 arcminute grid cell. A total of 485 grid cells across the study region had associated IgG serological data. Third, to ensure robust estimation of local FOI, we excluded all grid cells with fewer than 20 IgG assays from the analysis. Finally, we used the age-structured serological data from the 115 remaining grid cells (n = 3391 IgG serological assays) to estimate local FOI under the assumption that FOI was temporally constant within each grid cell [43]. Having obtained grid cell-level estimates of RVFV FOI, we then calculated the mean grid cell-level relative likelihood of interepidemic RVF from 2008 to 2022 using the model-based retrodictions previously described. We evaluated the significance of the relationship between estimated RVFV FOI and model-predicted interepidemic RVF likelihood using a linear model with FOI as the outcome, RVF likelihood as the predictor and the number of IgG serological assays conducted within each grid cell as a weight.

(c) Projecting interepidemic RVF risk under global change scenarios

To project future interepidemic RVF risk, we used the same set of 31 predictors previously described (electronic supplementary material, table S1). However, instead of weather data, we used statistically downscaled, 2.5 arcminute climate projections for three future time periods (2021–2040, 2041–2060, 2061–2080) under three climate scenarios (SSP126, SSP245, SSP370) (electronic supplementary material, 'Predictor Variables') to drive the model. Similarly, we used projections of human population density corresponding to the same time periods and underlying socioeconomic assumptions (i.e. SSP1, SSP2, SSP3) [44]. For each global change scenario, we developed multi-model risk projections across the study region for each month of the calendar year using the outputs of 11 different climate models from the Coupled Model Intercomparison Project (CMIP6; https://wcrp-cmip.org/cmip-phases/cmip6/). To summarize, in making risk projections, all static predictors were held constant, human population density varied according to the time period and SSP, and temperature and precipitation predictors varied according to the time period, SSP, climate model and calendar month. For comparison, we also retrodicted interepidemic RVF risk using historical climate (1970–2000) data and human population density data for the year 2000, which was the earliest year available.

(d) Estimating the human population at risk of interepidemic RVF under global change scenarios

Using our projected interepidemic RVF risk landscapes, we estimated the human population at risk of interepidemic RVF under future global change scenarios. This involved combining our risk projections with spatially explicit estimates of future human population density (electronic supplementary material, 'Predictor Variables') [44]. To define areas at risk of interepidemic RVF under a given future scenario, we thresholded all 12 monthly risk layers using the value that maximized the true skill statistic (TSS). These thresholded monthly risk layers delineated areas suitable for interepidemic RVF. We considered the human population in a given grid cell at risk of interepidemic RVF only if the cell was suitable for interepidemic RVF for

the majority of the calendar year (i.e. was suitable in >6 months). Using this method, we estimated the human population at risk of interepidemic RVF for all future scenarios described above. For comparison, we also estimated the human population at risk assuming historical climate (1970–2000) and human population density from the year 2000. Finally, to help parse the contributions of changing climate and changing human population to estimates of the future human population at risk of interepidemic RVF, we conducted sensitivity analyses using two alternative estimation methods (electronic supplementary material, table S2). First, we generated estimates of the human population at risk, assuming that climate changes according to the global change scenarios (SSP126, SSP245, SSP370) but that human population remains fixed at historical (year 2000) levels. Second, we generated estimates of the human population at risk assuming fixed historical (1970–2000) climate conditions but a changing human population, according to the global change scenarios (SSP1, SSP2, SSP3).

3. Results

(a) Modelling recent interepidemic RVF outbreaks

Model training produced a machine learning model with a mean AUC-ROC score of 0.74 (s.e. = 0.06) across the 11 training data folds. On withheld test data, the model had an AUC-ROC of 0.74 (electronic supplementary material, figure S2), indicating a good ability to distinguish RVF outbreak locations from background points. When model predictions were thresholded to maximize the TSS, the model had a TSS of 0.40, with a true negative rate (specificity) of 0.46 and a true positive rate (sensitivity) of 0.94 (electronic supplementary material, figure S2).

Variable importance for the 31 predictor variables in the model ranged from 0 to 0.13 (electronic supplementary material, figure S3). The 10 most important predictors included three precipitation variables, human population density, slope, soil clay content, soil pH, soil silt, goat density and elevation. Partial dependence plots (PDPs) showed that the relative likelihood of RVF generally decreases with human population density, slope and elevation but increases with soil pH, soil silt and goat density (electronic supplementary material, figure S4). The relationship between RVF and soil clay content was more complex and nonlinear (electronic supplementary material, figure S4). No temperature variable ranked higher than 12th in variable importance (electronic supplementary material, figure S3), but PDPs suggested temperature dependencies for interepidemic RVF. Monthly mean minimum temperatures of >20°C tended to increase disease risk, while monthly mean maximum temperatures >30°C decreased risk (electronic supplementary material, figure S4).

Of special note, three precipitation variables appeared in the top 10 most important predictors: monthly precipitation in the month of the event, monthly precipitation one month prior and monthly precipitation two months prior (electronic supplementary material, figure S3). Interestingly, PDPs revealed that precipitation in the month of the event was negatively related to interepidemic RVF risk but that the lagged precipitation variables were generally positively related to risk (electronic supplementary material, figure S4). While it was less important for prediction, cumulative precipitation in the three months prior to the event was also positively related to RVF (electronic supplementary material, figure S4).

(b) Independent model validation

Retrodictions of interepidemic RVF relative likelihood generated using our machine learning model were significantly predictive of spatially explicit RVFV FOI estimates derived from human serosurvey data (β = 0.014, s.e. = 0.002, $p < 0.001$, adjusted R^2 = 0.21; electronic supplementary material, figure S5).

(c) The recent risk landscape for interepidemic RVF

Model-based retrodictions allowed us to examine temporal and spatial patterns in recent interepidemic RVF risk across the study region. Despite year-to-year variation, retrodictions showed clear intra-annual seasonal patterns, with the relative likelihood of RVF tending to peak during May–July at the end of the long rains season (March–May) (figure 2). Likelihood of interepidemic RVF was predicted to be consistently low in August–November but was more variable in January and February following the cessation of the short rains (October–December) (figure 2). Interepidemic RVF risk was concentrated in low- and mid-elevation areas of Kenya (north and east) and Tanzania (northeast and southeast) (figure 2; electronic supplementary material, figure S6). There were also notable hotspots of RVF risk in southwest Uganda and, to its the south, the adjacent Kagera Region of Tanzania (electronic supplementary material, figure S6). Furthermore, some high-risk areas for RVF emerged in association with hydrological features. For example, the Kyela District (Mbeya Region) of Tanzania north of Lake Malawi, the Ntoroko District of Uganda bordering Lake Albert and portions of Uganda's Northern Region along the Albert Nile river all showed elevated disease risk (electronic supplementary material, figure S6). Lower risk of interepidemic RVF was predicted for the high-elevation inland areas of central and west Kenya as well as substantial swaths of west Tanzania, centred on the Tabora and Shinyanga Regions (electronic supplementary material, figure S6). During the short rains season (October–December), RVF risk was noticeably reduced across much of Tanzania (figure 2). Conversely, during the short rains season and immediately thereafter (January–March), the risk landscape in Uganda broadened beyond the country's primary hotspot in the southwest to include larger portions of the Central, Eastern and Northern Regions (figure 2).

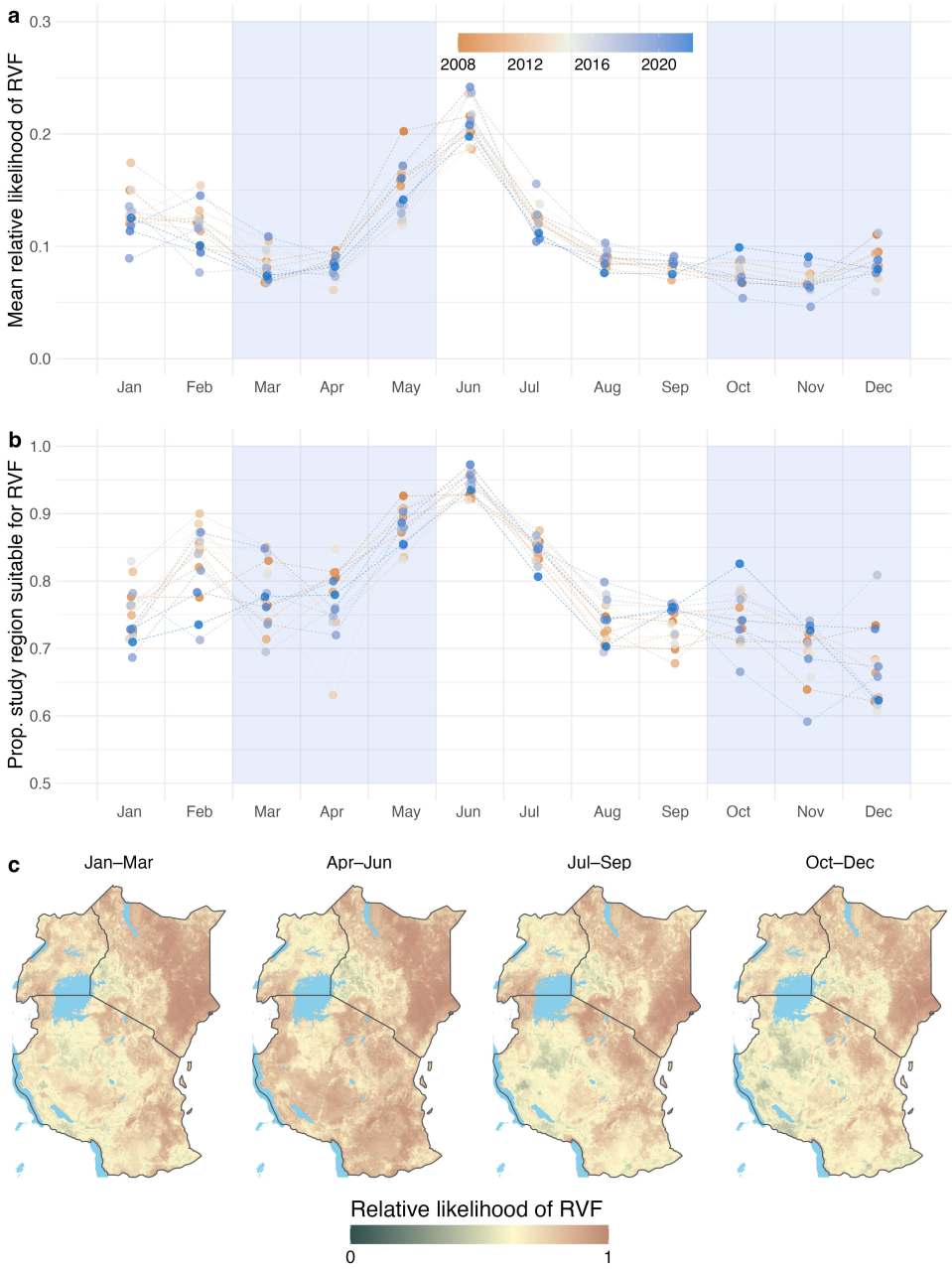

Figure 2. Temporal and spatial patterns in recent interepidemic RVF risk. Using the fit machine learning model, we retrodicted interepidemic RVF risk for every month from 2008 to 2022. We summarized model predictions into either the mean relative likelihood of interepidemic RVF across the study region (a) or the proportion of the study region suitable for RVF when model predictions were thresholded to maximize the true skill statistic (b). The colour bar for (a) and (b) indicates year, with orange representing earlier years and blue representing more recent years. Blue-shaded regions in (a) and (b) represent the long rains (March–May) and short rains (October–December) seasons. We also grouped retrodictions by months and averaged across all years from 2008 to 2022 to produce seasonal risk maps (c). In these maps, we plotted predictions on a $\log_{10}$ scale to better emphasize areas of intermediate risk. For the colour bar in (c), dark green corresponds to low relative likelihood of interepidemic RVF, while dark red corresponds to high likelihood. The colour bar was constructed such that yellow corresponds to the model's threshold value. In other words, yellow areas represent regions that are on the threshold of suitability for interepidemic RVF.

(d) Projecting interepidemic RVF risk under global change scenarios

Projections of interepidemic RVF risk under expected mid- and late-twenty-first century climate and human population distribution also showed seasonality (figure 3a), but with some change relative to historical conditions (electronic supplementary material, figures S6 and S7). Most notably, there was decreased RVF risk across most of the calendar year, apart from March to May. The risk decrease relative to historical conditions was particularly apparent in later time periods (i.e. 2061–2080) under the high-radiative forcing, high-population SSP370 scenario (figure 3a). This trend was largely attributable to expected risk decreases over time in portions of east Kenya, northeast Tanzania and southwest Uganda (electronic supplementary material, figures S6–S16).

Although mean RVF risk generally decreases when comparing future scenarios with historical conditions (figure 3a), this overall trend disguised opposing changes in different parts of the study region. For example, large decreases in expected risk in the eastern extremes of Kenya were partially offset by increases in expected risk across a more interior strip running from

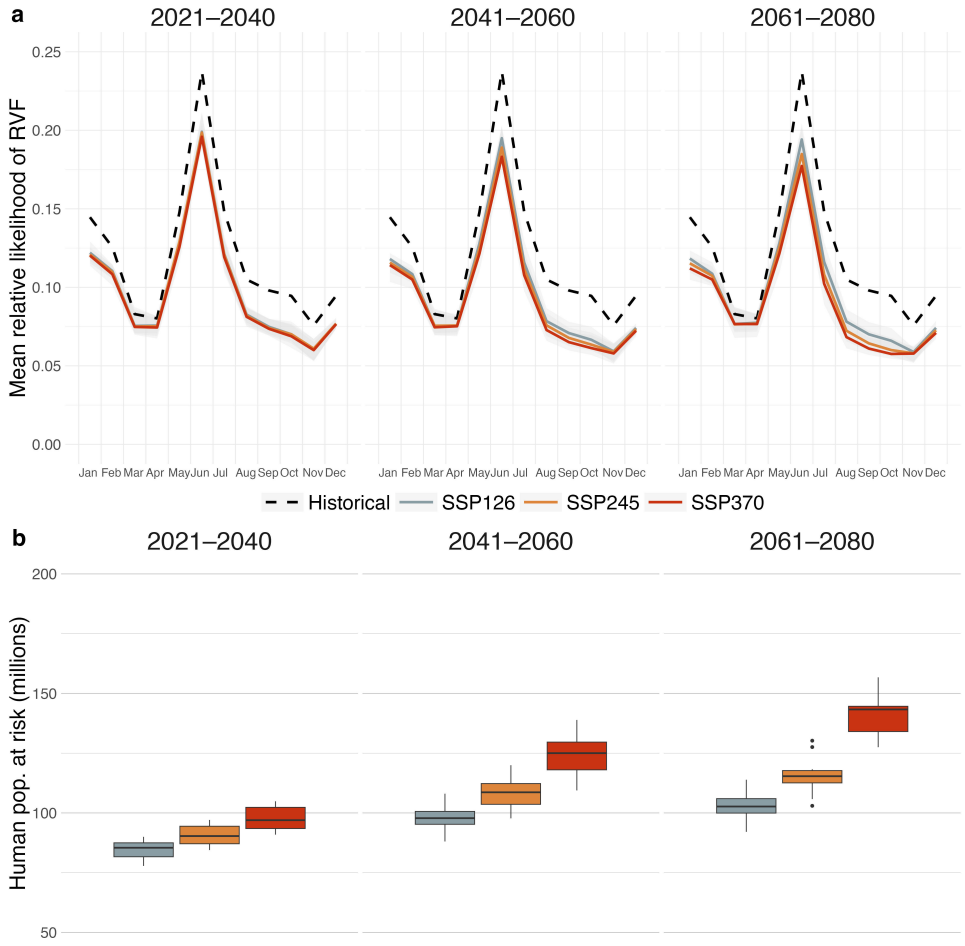

Figure 3. Projected future interepidemic RVF risk and corresponding human population at risk. Using the fit machine learning model, we predicted RVF risk under both historical (1970–2000) and future conditions (a). The mean monthly predictions for the single historical climate scenario are shown as a dashed black line in each panel facet to provide a consistent basis for comparison. Projections under future conditions were generated for 3 time periods (panel columns), 3 paired climate and human population scenarios (line colour) and 11 climate models. The solid lines within each panel facet correspond to the multi-model mean across the 11 climate models, while the grey-shaded regions indicate the range of risk projections across climate models. These multi-model risk projections were combined with projections of human population density to estimate the human population exposed to interepidemic RVF for the majority of the calendar year under each future scenario (b).

Marsabit County in the north through Tana River County in the south (electronic supplementary material, figures S6–S16). In Tanzania, portions of the southerly Morogoro, Lindi and Ruvuma Regions may increase in risk even as large portions of the country's northeast and northwest become less risky over time (electronic supplementary material, figures S6–S16). Across Uganda, the future risk landscape for interepidemic RVF is mostly expected to decrease relative to historical conditions, especially in the country's southwest near the border with Tanzania (electronic supplementary material, figures S6–S16). However, in some calendar months, risk is projected to increase in the areas along Lake Albert and the Albert Nile river in western Uganda (electronic supplementary material, figures S8–S16).

(e) Estimating the human population at risk of interepidemic RVF under global change scenarios

We estimated that under historical climate and human population distribution, approximately 49 million people throughout the study region lived in areas with high interepidemic RVF risk for most of the calendar year (electronic supplementary material, table S2). Despite projected decreases in mean RVF risk across the study region under all global change scenarios (figure 3a), concomitant increases in the expected human population translate to increasingly large numbers of people exposed to interepidemic RVF under future conditions (figure 3b). By 2061–2080, we estimate that approximately 92–157 million people throughout the study region will be living in areas with high interepidemic RVF risk for most of the year (figure 3b; electronic supplementary material, table S2). However, population exposure to RVF was highest under the SSP370 scenario: all estimates for 2061–2080 and this global change scenario indicated >127 million people at risk, which is more than double the historical estimate.

Sensitivity analyses clarified the dominant role that projected human population growth plays in driving elevated estimates of the future human population at risk from RVF. If we use future climate scenarios but fix human population at historical (year 2000) levels, estimates of the human population at risk from interepidemic RVF throughout the twenty-first century are lower than the historical estimate of 49 million and decrease over time (electronic supplementary material, table S2 and figure S17). Conversely, if we assume a fixed, historical climate (1970–2000) but allow future human population to change according to the SSP scenarios, estimates of the future human population at risk are higher than the analogous estimates that assume concurrent change to both climate and human population (electronic supplementary material, table S2 and figure S17).

4. Discussion

We developed and validated a machine learning model of interepidemic RVF that predicted seasonal and spatial variation in disease risk across Kenya, Tanzania and Uganda. When used to project future RVF risk, the model suggested that risk will largely decrease relative to historical conditions. Despite an expected mean decrease in disease risk across the study region, we recover a shifting risk landscape, with certain areas becoming more suitable for interepidemic RVF as others become less suitable. Furthermore, given expected human population growth, we predict that > 90 million people in the study region will be exposed to interepidemic RVF for the majority of each calendar year by 2061–2080. Our results underscore the threat that RVF could pose to public health across East Africa in the coming decades and simultaneously improve our ability to monitor and mitigate disease risk.

(a) Interepidemic RVF model performance and validation

Before discussing our results in more detail, we note that our machine learning model of interepidemic RVF had very high sensitivity (0.94) but relatively low specificity (0.46) when applied to the test dataset of outbreak and background points from 2019 to 2022. The model's high sensitivity indicates that most known outbreak points are accurately classified, suggesting that true high-risk locations and time periods are likely to appear as high-risk in our analyses. This is a desirable property allowing the prioritization of future RVF surveillance and mitigation activities. Simultaneously, we caution that the model's low specificity indicates that some signals of elevated risk in our analyses may be false positives.

In support of our model's robustness, predictions of RVF relative likelihood were positively correlated with completely independent estimates of RVFV FOI into humans. This suggests that our model, which was trained solely on RVF outbreak location data (including cases in both livestock and humans), captures important processes driving human exposure to RVFV. One caveat is that our method for estimating FOI, which relies on age-structured IgG serological data, assumes that FOI has been constant for as long as the oldest individual in the dataset has been alive (approximately 90 years) [43]. Because RVFV FOI changes substantially during the transition between epidemic and interepidemic regimes and is likely to vary over time even within interepidemic periods, this assumption cannot hold in a literal sense. Despite this limitation, the fact that we recovered a significant positive relationship between model predictions and estimated FOI suggests that similar processes shape the long-term average risk of RVFV exposure across both interepidemic and epidemic periods. More robust validation of our machine learning predictions, which are made at the monthly timescale, would require reconstructing historical FOI by coupling serological data to more complex mathematical models that allow FOI to vary over time.

(b) Drivers of interepidemic RVF risk

Our model indicated that precipitation, human population density, soil characteristics, slope, elevation and goat density were the most important predictors of interepidemic RVF. With respect to precipitation, we found that interepidemic RVF outbreaks were more likely to occur in relatively dry months that were preceded by wet months (i.e. months near the end of rainy seasons). As such, there was distinct seasonality in predicted interepidemic RVF risk, with elevated risk May–July following the long rains season (March–May) and a secondary peak January–February following the short rains season (October–December). These findings agree with prior work on the timing of RVF outbreaks [23] and are unsurprising given the key role that precipitation plays in the growth of RVFV vector populations [3,4,22,24]. Previous studies also found, as we did, that certain soil types and lower elevations are associated with RVF [22,24,45]. These environments likely represent optimal habitat for RVFV vectors and cryptic RVFV circulation. Interestingly, goat density was the most important livestock predictor of interepidemic RVF, with higher goat densities driving increased disease risk. This relationship deserves further investigation, but our work adds to existing evidence that goats may be important sentinels of RVF risk in humans [46,47].

Notably, RVF outbreak risk was negatively related to human population density in our model. We emphasize that the background points used in model training were themselves drawn in proportion to human population density. Discovery and reporting biases are pervasive throughout disease ecology [48–50], and reporting can be a major factor shaping the observed distribution of disease events [51], including in the RVF system [23,52]. This motivated our approach to background point selection, which was meant to minimize the influence of disease reporting bias [35], under the assumption that disease surveillance and reporting effort scale with human population density. From a biological perspective, it is feasible that RVF risk is reduced in areas with dense human settlements. There is little evidence for human-to-human transmission of RVFV, and human cases are most likely to be acquired through contact with mosquito vectors or exposure to infected animals [1,53]. As such, it may be that there is lower risk of RVFV maintenance and transmission in dense urban centres compared with rural areas with limited vector control, higher livestock densities and greater human–livestock interaction. Indeed, the predictor data used here indicate that areas of dense human population (i.e. > 5000 people per km^2) tend to have limited livestock densities, which presumably reduces the opportunity for RVFV exposure.

(c) Spatial variation in interepidemic RVF risk

Our model predicted substantial spatial variation in interepidemic RVF risk across the study region, and this heterogeneous risk landscape is largely expected to persist with global change. Large portions of low-elevation east Kenya were predicted to be at high risk of interepidemic RVF, including the counties of Marsabit, Isiolo, Tana River, Taita-Taveta, Lamu, Garissa, Wajir

and Mandera. These findings are congruent with prior work demonstrating elevated RVF risk in many of these same areas [13,14,22,24]. Crucially, because of our background data selection methods, our model could identify these sparsely populated areas as high-risk despite limited disease reporting in some counties. Similarly, our dataset contained no interepidemic RVF outbreak events from Turkana County in northwest Kenya, yet our model predicted high suitability for interepidemic RVF in this known high-risk region [12,14]. In Tanzania, interepidemic RVF risk was concentrated in (i) portions of the northeast, namely, the Mara, Simiyu, Arusha and Manyara Regions, (ii) low-elevation coastal and inland areas of the southeast, namely the Morogoro, Pwani and Lindi Regions, and (iii) the western Kagera Region bordering Uganda. We also recovered a notable RVF hotspot immediately north of Lake Malawi in the Kyela District (Mbeya Region), mirroring prior work [15]. Human RVFV IgG seroprevalence can approach 30% in the low-lying areas adjacent to Lake Malawi [15], and this part of Tanzania deserves special attention as a site of endemic RVFV circulation [45,54]. Finally, in Uganda, our model suggested high risk in the country's southwest, an area that is probably an epicentre for RVFV transmission [18,19,55,56], as well as in the west near Lake Albert and the Albert Nile river. Collectively, our results highlight regions to prioritize for RVF surveillance and mitigation, both now and in the future.

(d) Interepidemic RVF risk under global change scenarios

Projections of interepidemic RVF showed broad risk decreases in response to anticipated changes in climate and human population. This risk decrease scaled with global change scenario, being most pronounced in the high-radiative forcing, high-population SSP370 scenario towards the end of the twenty-first century. Spatially, this trend manifested most clearly in the Kenyan counties of Mandera, Wajir and Garissa, suggesting that future climatic changes and shifting human populations will create less favourable conditions for RVF in these arid, low-elevation environments. We emphasize that even with expected risk decreases owing to global change, these areas will remain high-risk relative to much of the study region. In Tanzania, a primary finding from our global change modelling was that a decrease in RVF risk in the northeast may be accompanied by an increase in RVF risk in the south. Specifically, an area centred on the southern Morogoro Region is projected to experience RVF risk increases during March–May (electronic supplementary material, figures S8–S16). The Morogoro Region, which we predict is already at high risk of interepidemic RVF, deserves increased public health attention. Finally, in Uganda, the main projected change in future interepidemic RVF risk was a risk reduction in the southwest. Interestingly, projected risk reductions in this area are a continuation of changes to the risk landscape that are already underway: our retrodictions for 2008–2022 show slightly decreased risk in southwest Uganda when compared with predictions made under historical 1970–2000 climate (electronic supplementary material, figure S6). We stress that southwest Uganda remains a relatively high-risk area within the broader study region, even accounting for projected risk decreases. However, our modelling also suggests that the areas surrounding Lake Albert may emerge as an important site for RVFV transmission in Uganda in the future.

Our interepidemic RVF risk projections assumed changing precipitation, temperature and human population density, and, of these three, precipitation is arguably the factor that is both most important to RVF epidemiology and most uncertain. Temperature showed a relatively straightforward relationship with RVF in that low minimum temperatures and high maximum temperatures both reduced predicted disease risk. Because the SSP scenarios uniformly imply warming across the study region (albeit to varying degrees in different scenarios) [57], temperature changes influence future interepidemic RVF risk to the extent that areas warm into or out of the disease's optimal thermal range. Similarly, human population density had a simple estimated relationship with interepidemic RVF in that greater densities reduced disease risk. Because all SSP scenarios assume a growing human population in the study region throughout the twenty-first century [44], future population trends broadly serve to decrease RVF risk. By contrast, precipitation had a more complex relationship with interepidemic RVF: disease risk increased in relatively dry months that were preceded by wet months (electronic supplementary material, figure S4). As such, our projections of interepidemic RVF risk are affected by both the magnitude and timing of expected precipitation.

Given that our disease projections are sensitive to precipitation inputs, we stress the need for more trustworthy precipitation projections, a predictive task that is currently subject to numerous uncertainties [57,58]. Importantly, while our study region of central East Africa is projected to undergo a moderate wetting trend throughout the twenty-first century, other parts of Africa could receive even larger proportional increases in precipitation (e.g. north East Africa, central Africa) or, alternatively, could experience drying (e.g. south Africa) [57]. Thus, the impacts of climate change on interepidemic RVF in these regions may differ from what we project in central East Africa. Beyond simple wetting or drying trends, accurate projections across Africa of change in precipitation frequency, duration and intensity, including extreme events that lead to flooding, will be key to skillful projections of future RVF risk. For example, in East Africa, increased precipitation in historically dry months (e.g. July–September) [58] could generate RVF disease dynamics that depart from established seasonal regimes.

(e) Human population at risk of interepidemic RVF under global change scenarios

Because all SSP scenarios assume human population growth in the study region, we estimate that increasing numbers of people will be exposed to interepidemic RVF throughout the twenty-first century, even despite projected decreases in average disease risk across the landscape (electronic supplementary material, table S2). Our sensitivity analyses demonstrated that changing climate and changing human population distribution have counteracting influences on the future human population at risk from RVF. For example, relative to our primary estimates of the human population at risk, which were generated using both future climate and future human population projections, alternative estimates generated assuming static, historical climate conditions and future human population change show even larger numbers of people at risk (electronic supplementary

material, figure S17). In other words, future climate regimes are expected to decrease landscape-scale suitability for RVF, partly mitigating the health burden that would be expected owing to a growing human population alone.

(f) Epidemic or hyperendemic RVFV dynamics in East Africa?

In this work, we adopted the classical view of RVF epidemiology based on epidemic disease dynamics. Under this model, sporadic RVF epidemics, which are typified by explosive case counts (in both livestock and humans) and disease spread over large areas, are interspersed with interepidemic periods characterized by more limited disease transmission [10,12,59]. Given that the major 2006–2007 RVF outbreak in East Africa is widely recognized as an epidemic event [60–62], we collated East African RVF outbreak data after 2007 as representative of interepidemic cases, ultimately generating a dataset that spanned 2008–2022.

We acknowledge that the interepidemic status of the year 2018 may be questionable: relatively large numbers of RVF cases were observed that year, including the largest annual RVF case counts in humans across our 2008–2022 dataset for Kenya [63], Tanzania [64–66] and Uganda [21]. However, the fact that RVF surveillance effort has varied substantially over time greatly complicates interpretation of RVFV dynamics. For example, elevated RVF case counts in Uganda in 2018 may be at least partially attributable to increased surveillance capacity (given the creation of the country's viral haemorrhagic fever surveillance programme in 2010 [21,67]) coupled with heightened interest in RVF surveillance (owing to the first detection of RVF cases in Uganda in 2016 after a multi-decade absence [18,19]). Furthermore, many acute human RVF cases in Tanzania in 2018 were documented via cross-sectional sampling for viral haemorrhagic fevers that happened to occur from June to November 2018 [64,65], leaving open the possibility that a similar sampling scheme deployed in other years might have captured similar numbers of RVF cases. For these reasons, we ultimately chose to consider all outbreak data from 2008 to 2022 as deriving from interepidemic rather than epidemic transmission.

Nonetheless, the observed variation in outbreak number and case counts across years highlights the complexity of RVFV dynamics. In fact, Rostal *et al.* [59] recently proposed that RVF epidemiology may break from the traditional epidemic model in some parts of Africa. Rather than classical epidemic–interepidemic cycles, there may instead be a hyperendemic RVFV dynamic characterized by sustained RVFV transmission and relatively high disease incidence or prevalence. Indeed, portions of our East African study region might maintain RVFV in a hyperendemic pattern [56], and we echo calls for further work that could help clarify whether some RVF disease events currently considered interepidemic cases by the RVF research community are better described as arising from hyperendemic transmission [59].

5. Conclusions

In sum, our interepidemic RVF model showed seasonally varying disease risk, with the highest RVF risk during May–July. Disease risk is generally projected to decrease under future global change scenarios. Despite expected risk decreases, when coupled with projections of human population growth, these predictions suggest that >90 million people in the study region may be exposed to interepidemic RVF by 2061–2080. Consequently, we urge increased disease surveillance, prevention and control efforts in the geographic areas we identify as high-risk. In addition, focused studies are needed to help differentiate East African regions experiencing epidemic versus hyperendemic RVFV dynamics [59], and further work at the animal–human interface would clarify the specific conditions that lead to human RVFV exposure. Finally, targeted public health interventions, such as vaccination campaigns informed by predictive models, could help mitigate the animal and human health impacts of RVF in a changing world [68].

Ethics. Data access and usage were reviewed and approved by the Kenyatta National Hospital—University of Nairobi ethical review committee (KNH-UoN ERC P810/10/2022) for Kenya. Protocols for the collection of serological data were approved by the Scientific and Ethics Review Unit of the Kenya Medical Research Institute (KEMRI/SERU/CGHR/4169). Uganda data access and use were approved by the Uganda Ministry of Health. Data for Tanzania were obtained from published literature. At the request of data providers, serological data are not shared with granular information on patient age and location to preserve privacy.

Data accessibility. Data and code are available on Zenodo [33].

Supplementary material is available online [69].

Declaration of AI use. We have not used AI-assisted technologies in creating this article.

Authors' contributions. E.A.E.: conceptualization, data curation, formal analysis, methodology, validation, writing—original draft; E.C.: conceptualization, data curation, methodology, validation, writing—review and editing; D.S.: conceptualization, methodology, writing—review and editing; S.S.: data curation, methodology, writing—review and editing; L.N.: data curation, methodology, writing—review and editing; M.K.N.: conceptualization, funding acquisition, methodology, project administration, supervision, writing—review and editing; S.L.N.: conceptualization, funding acquisition, methodology, project administration, supervision, validation, writing—review and editing.

All authors gave final approval for publication and agreed to be held accountable for the work performed therein.

Conflict of interest declaration. We declare we have no competing interests.

Funding. Funding for this project was provided by the Coalition for Epidemic Preparedness Innovations (CEPI) through the 'Epidemiology and modelling studies to support Rift Valley fever vaccine efficacy trials in East Africa' project to M.K.N., by the US National Institute of Allergy and Infectious Diseases/National Institutes of Health (NIAID/NIH) grant number U01AI151799 through the Center for Research in Emerging Infectious Diseases-East and Central Africa (CREID-ECA) to M.K.N. and by the US National Institute of General Medical Sciences/National Institutes of Health (NIGMS/NIH) grant number R01GM122079 to S.L.N.

Acknowledgements. Serological data and metadata were provided by the University of Glasgow and were generated through the Zoonoses and Emerging Livestock Systems programme funded by the UK Biotechnology and Biological Sciences Research Council (BB/L018926/1 and BB/J010367).

References

1. McMillen CM, Hartman AL. 2018 Rift Valley fever in animals and humans: current perspectives. *Antivir. Res*. **156**, 29–37. (doi:10.1016/j.antiviral.2018.05.009)
2. Nanyingi MO, Munyua P, Kiama SG, Muchemi GM, Thumbi SM, Bitek AO, Bett B, Muriithi RM, Njenga MK. 2015 A systematic review of Rift Valley Fever epidemiology 1931–2014. *Infect. Ecol. Epidemiol*. **5**, 28024. (doi:10.3402/iee.v5.28024)
3. Davies FG, Linthicum KJ, James AD. 1985 Rainfall and epizootic Rift Valley fever. *Bull. World Health Organ*. **63**, 941–943.
4. Williams R, Malherbe J, Weepener H, Majiwa P, Swanepoel R. 2016 Anomalous high rainfall and soil saturation as combined risk indicator of Rift Valley fever outbreaks, South Africa, 2008–2011. *Emerg. Infect. Dis*. **22**, 2054–2062. (doi:10.3201/eid2212.151352)
5. Martin V, Chevalier V, Ceccato P, Anyamba A, De Simone L, Lubroth J, de La Rocque S, Domenech J. 2008 The impact of climate change on the epidemiology and control of Rift Valley fever. *Rev. Sci. Tech. Off. Int. Epizoot* **27**, 413–426. (doi:10.20506/rst.27.2.1802)
6. Murithi RM, Munyua P, Ithondeka PM, Macharia JM, Hightower A, Luman ET, Breiman RF, Njenga MK. 2011 Rift Valley fever in Kenya: history of epizootics and identification of vulnerable districts. *Epidemiol. Infect*. **139**, 372–380. (doi:10.1017/S0950268810001020)
7. Linthicum KJ, Bailey CL, Davies FG, Tucker CJ. 1987 Detection of Rift Valley fever viral activity in Kenya by satellite remote sensing imagery. *Science* **235**, 1656–1659. (doi:10.1126/science.3823909)
8. Linthicum KJ, Anyamba A, Tucker CJ, Kelley PW, Myers MF, Peters CJ. 1999 Climate and satellite indicators to forecast Rift Valley fever epidemics in Kenya. *Science* **285**, 397–400. (doi:10.1126/science.285.5426.397)
9. Anyamba A *et al*. 2009 Prediction of a Rift Valley fever outbreak. *Proc. Natl Acad. Sci. USA* **106**, 955–959. (doi:10.1073/pnas.0806490106)
10. Njenga MK, Bett B. 2019 Rift Valley fever virus—how and where virus is maintained during inter-epidemic periods. *Curr. Clin. Microbiol. Rep*. **6**, 18–24. (doi:10.1007/s40588-018-0110-1)
11. Rostal MK *et al*. 2025 Localized Rift Valley fever virus persistence explains epidemic and interepidemic dynamics and guides control strategies. *Proc. R. Soc. B* **292**, 20250453. (doi:10.1098/rspb.2025.0453)
12. LaBeaud AD, Ochiai Y, Peters CJ, Muchiri EM, King CH. 2007 Spectrum of Rift Valley fever virus transmission in Kenya: insights from three distinct regions. *Am. J. Trop. Med. Hyg* **76**, 795–800. (doi:10.4269/ajtmh.2007.76.795)
13. LaBeaud AD, Muchiri EM, Ndzovu M, Mwanje MT, Muiruri S, Peters CJ, King CH. 2008 Interepidemic Rift Valley fever virus seropositivity, northeastern Kenya. *Emerg. Infect. Dis*. **14**, 1240–1246. (doi:10.3201/eid1408.080082)
14. Muiruri S, Kabiru EW, Muchiri EM, Hussein H, Kagondu F, LaBeaud AD, King CH. 2015 Cross-sectional survey of Rift Valley fever virus exposure in Bodhei Village located in a transitional coastal forest habitat in Lamu County, Kenya. *Am. J. Trop. Med. Hyg*. **92**, 394–400. (doi:10.4269/ajtmh.14-0440)
15. Heinrich N *et al*. 2012 High seroprevalence of Rift Valley fever and evidence for endemic circulation in Mbeya region, Tanzania, in a cross-sectional study. *PLoS Neglected Trop. Dis*. **6**, e1557. (doi:10.1371/journal.pntd.0001557)
16. Sumaye RD, Abatih EN, Thiry E, Amuri M, Berkvens D, Geubbels E. 2015 Inter-epidemic acquisition of Rift Valley fever virus in humans in Tanzania. *PLoS Neglected Trop. Dis*. **9**, e0003536. (doi:10.1371/journal.pntd.0003536)
17. de Glanville WA *et al*. 2022 Inter-epidemic Rift Valley fever virus infection incidence and risks for zoonotic spillover in northern Tanzania. *PLoS Neglected Trop. Dis*. **16**, e0010871. (doi:10.1371/journal.pntd.0010871)
18. Nyakarahuka L *et al*. 2018 Prevalence and risk factors of Rift Valley fever in humans and animals from Kabale district in Southwestern Uganda, 2016. *PLoS Neglected Trop. Dis*. **12**, e0006412. (doi:10.1371/journal.pntd.0006412)
19. Shoemaker TR *et al*. 2019 First laboratory-confirmed outbreak of human and animal Rift Valley fever virus in Uganda in 48 years. *Am. J. Trop. Med. Hyg*. **100**, 659–671. (doi:10.4269/ajtmh.18-0732)
20. Cossaboom CM *et al*. 2022 Rift Valley fever outbreak during COVID-19 surge, Uganda, 2021. *Emerg. Infect. Dis*. **28**, 2290–2293. (doi:10.3201/eid2811.220364)
21. Nyakarahuka L *et al*. 2023 Detection of sporadic outbreaks of Rift Valley fever in Uganda through the national viral hemorrhagic fever surveillance system, 2017–2020. *Am. J. Trop. Med. Hyg*. **108**, 995–1002. (doi:10.4269/ajtmh.22-0410)
22. Hightower A *et al*. 2012 Relationship of climate, geography, and geology to the incidence of Rift Valley fever in Kenya during the 2006–2007 outbreak. *Am. J. Trop. Med. Hyg*. **86**, 373–380. (doi:10.4269/ajtmh.2012.11-0450)
23. Sindato C, Karimuribo ED, Pfeiffer DU, Mboera LEG, Kivaria F, Dautu G, Bernard B, Paweska JT. 2014 Spatial and temporal pattern of Rift Valley fever outbreaks in Tanzania; 1930 to 2007. *PLoS One* **9**, e88897. (doi:10.1371/journal.pone.0088897)
24. Munyua PM *et al*. 2016 Predictive factors and risk mapping for Rift Valley fever epidemics in Kenya. *PLoS One* **11**, e0144570. (doi:10.1371/journal.pone.0144570)
25. Baker RE *et al*. 2022 Infectious disease in an era of global change. *Nat. Rev. Microbiol*. **20**, 193–205. (doi:10.1038/s41579-021-00639-z)
26. Carlson CJ, Albery GF, Merow C, Trisos CH, Zipfel CM, Eskew EA, Olival KJ, Ross N, Bansal S. 2022 Climate change increases cross-species viral transmission risk. *Nature* **607**, 555–562. (doi:10.1038/s41586-022-04788-w)
27. Mora C *et al*. 2022 Over half of known human pathogenic diseases can be aggravated by climate change. *Nat. Clim. Chang*. **12**, 869–875. (doi:10.1038/s41558-022-01426-1)
28. de Souza WM, Weaver SC. 2024 Effects of climate change and human activities on vector-borne diseases. *Nat. Rev. Microbiol*. **22**, 476–491. (doi:10.1038/s41579-024-01026-0)
29. Taylor D, Hagenlocher M, Jones AE, Kienberger S, Leedale J, Morse AP. 2016 Environmental change and Rift Valley fever in eastern Africa: projecting beyond HEALTHY FUTURES. *Geospat. Health* **11**, 387. (doi:10.4081/gh.2016.387)
30. Mweya CN, Mboera LEG, Kimera SI. 2017 Climate influence on emerging risk areas for Rift Valley fever epidemics in Tanzania. *Am. J. Trop. Med. Hyg*. **97**, 109–114. (doi:10.4269/ajtmh.16-0444)
31. Situma S *et al*. 2024 Widening geographic range of Rift Valley fever disease clusters associated with climate change in East Africa. *BMJ Glob. Health* **9**, e014737. (doi:10.1136/bmjgh-2023-014737)
32. Skinner EB, Glidden CK, MacDonald AJ, Mordecai EA. 2023 Human footprint is associated with shifts in the assemblages of major vector-borne diseases. *Nat. Sustain*. **6**, 652–661. (doi:10.1038/s41893-023-01080-1)
33. Eskew EA, Clancey E, Singh D, Situma S, Nyakarahuka L, Njenga MK, Nuismer SL. 2025 Data and code supporting analyses of interepidemic Rift Valley fever risk in East Africa (Version 1.0.0). Zenodo. (doi:10.5281/zenodo.17582924)
34. Meisner J *et al*. 2025 Mapping hotspots of zoonotic pathogen emergence: an integrated model-based and participatory-based approach. *Lancet Planet. Health* **9**, e14–e22. (doi:10.1016/S2542-5196(24)00309-7)

35. Gibb R *et al*. 2024 The anthropogenic fingerprint on emerging infectious diseases. *medRxiv* 2024.05.22.24307684. (doi:10.1101/2024.05.22.24307684)
36. Chen T, Guestrin C. 2016 XGBoost: a scalable tree boosting system. In *Proc. of the 22nd ACM SIGKDD International Conference on Knowledge Discovery and Data Mining*, pp. 785–794. New York, NY: Association for Computing Machinery. (doi:10.1145/2939672.2939785)
37. Valavi R, Guillera-Arroita G, Lahoz-Monfort JJ, Elith J. 2022 Predictive performance of presence-only species distribution models: a benchmark study with reproducible code. *Ecol. Monogr*. **92**, e01486. (doi:10.1002/ecm.1486)
38. Richardson E, Trevizani R, Greenbaum JA, Carter H, Nielsen M, Peters B. 2024 The receiver operating characteristic curve accurately assesses imbalanced datasets. *Patterns* **5**, 100994. (doi:10.1016/j.patter.2024.100994)
39. Valavi R, Elith J, Lahoz-Monfort JJ, Guillera-Arroita G. 2021 Modelling species presence-only data with random forests. *Ecography* **44**, 1731–1742. (doi:10.1111/ecog.05615)
40. R Core Team. 2024 R: a language and environment for statistical computing. Vienna, Austria: R Foundation for Statistical Computing. See https://www.R-project.org/.
41. Kuhn M, Silge J. 2022 *Tidy Modeling with R: A Framework for Modeling in the Tidyverse*. Sebastopol, CA: O'Reilly Media, Inc.
42. Cook EAJ, Grossi-Soyster EN, de Glanville WA, Thomas LF, Kariuki S, Bronsvoort BM de C, Wamae CN, LaBeaud AD, Fèvre EM. 2017 The sero-epidemiology of Rift Valley fever in people in the Lake Victoria Basin of western Kenya. *PLoS Neglected Trop. Dis*. **11**, e0005731. (doi:10.1371/journal.pntd.0005731)
43. Heisey DM, Joly DO, Messier F. 2006 The fitting of general force-of-infection models to wildlife disease prevalence data. *Ecology* **87**, 2356–2365. (doi:10.1890/0012-9658(2006)87[2356:tfogfm]2.0.co;2)
44. Wang X, Meng X, Long Y. 2022 Projecting 1 km-grid population distributions from 2020 to 2100 globally under shared socioeconomic pathways. *Sci. Data* **9**, 563. (doi:10.1038/s41597-022-01675-x)
45. Sindato C, Pfeiffer DU, Karimuribo ED, Mboera LEG, Rweyemamu MM, Paweska JT. 2015 A spatial analysis of Rift Valley fever virus seropositivity in domestic ruminants in Tanzania. *PLoS One* **10**, e0131873. (doi:10.1371/journal.pone.0131873)
46. Gerken KN *et al*. 2022 Urban risk factors for human Rift Valley fever virus exposure in Kenya. *PLoS Glob. Public Health* **2**, e0000505. (doi:10.1371/journal.pgph.0000505)
47. Omani R *et al*. 2024 Goat seropositivity as an indicator of Rift Valley fever (RVF) infection in human populations: a case-control study of the 2018 Rift Valley fever outbreak in Wajir County, Kenya. *One Health* **19**, 100921. (doi:10.1016/j.onehlt.2024.100921)
48. Allen T, Murray KA, Zambrana-Torrelio C, Morse SS, Rondinini C, Di Marco M, Breit N, Olival KJ, Daszak P. 2017 Global hotspots and correlates of emerging zoonotic diseases. *Nat. Commun*. **8**, 1124. (doi:10.1038/s41467-017-00923-8)
49. Albery GF, Carlson CJ, Cohen LE, Eskew EA, Gibb R, Ryan SJ, Sweeny AR, Becker DJ. 2022 Urban-adapted mammal species have more known pathogens. *Nat. Ecol. Evol*. **6**, 794–801. (doi:10.1038/s41559-022-01723-0)
50. Gibb R, Albery GF, Mollentze N, Eskew EA, Brierley L, Ryan SJ, Seifert SN, Carlson CJ. 2022 Mammal virus diversity estimates are unstable due to accelerating discovery effort. *Biol. Lett.* **18**, 20210427. (doi:10.1098/rsbl.2021.0427)
51. Redding DW *et al*. 2021 Geographical drivers and climate-linked dynamics of Lassa fever in Nigeria. *Nat. Commun*. **12**, 5759. (doi:10.1038/s41467-021-25910-y)
52. Sindato C, Stevens KB, Karimuribo ED, Mboera LEG, Paweska JT, Pfeiffer DU. 2016 Spatial heterogeneity of habitat suitability for Rift Valley fever occurrence in Tanzania: an ecological niche modelling approach. *PLoS Neglected Trop. Dis*. **10**, e0005002. (doi:10.1371/journal.pntd.0005002)
53. Al-Hamdan NA, Panackal AA, Al Bassam TH, Alrabea A, Al Hazmi M, Al Mazroa Y, Al Jefri M, Khan AS, Ksiazek TG. 2015 The risk of nosocomial transmission of Rift Valley fever. *PLoS Neglected Trop. Dis*. **9**, e0004314. (doi:10.1371/journal.pntd.0004314)
54. Matiko MK, Salekwa LP, Kasanga CJ, Kimera SI, Evander M, Nyangi WP. 2018 Serological evidence of inter-epizootic/inter-epidemic circulation of Rift Valley fever virus in domestic cattle in Kyela and Morogoro, Tanzania. *PLoS Neglected Trop. Dis*. **12**, e0006931. (doi:10.1371/journal.pntd.0006931)
55. Tumusiime D, Isingoma E, Tashoroora OB, Ndumu DB, Bahati M, Nantima N, Mugizi DR, Jost C, Bett B. 2023 Mapping the risk of Rift Valley fever in Uganda using national seroprevalence data from cattle, sheep and goats. *PLoS Neglected Trop. Dis*. **17**, e0010482. (doi:10.1371/journal.pntd.0010482)
56. Bakamutumaho B *et al*. 2025 Hyperendemicity of Rift Valley fever in Southwestern Uganda associated with the rapidly evolving lineage C viruses. *J. Infect. Dis.* jiaf417. (doi:10.1093/infdis/jiaf417)
57. Almazroui M, Saeed F, Saeed S, Nazrul Islam M, Ismail M, Klutse NAB, Siddiqui MH. 2020 Projected change in temperature and precipitation over Africa from CMIP6. *Earth Syst. Environ*. **4**, 455–475. (doi:10.1007/s41748-020-00161-x)
58. Palmer PI *et al*. 2023 Drivers and impacts of Eastern African rainfall variability. *Nat. Rev. Earth Environ*. **4**, 254–270. (doi:10.1038/s43017-023-00397-x)
59. Rostal MK *et al*. 2025 Rift Valley fever epidemiology: shifting the paradigm and rethinking research priorities. *Lancet Planet. Health* **9**, 101299. (doi:10.1016/j.lanplh.2025.101299)
60. Munyua P *et al*. 2010 Rift Valley fever outbreak in livestock in Kenya, 2006–2007. *Am. J. Trop. Med. Hyg*. **83**, 58–64. (doi:10.4269/ajtmh.2010.09-0292)
61. Nguku PM *et al*. 2010 An investigation of a major outbreak of Rift Valley fever in Kenya: 2006–2007. *Am. J. Trop. Med. Hyg*. **83**, 5–13. (doi:10.4269/ajtmh.2010.09-0288)
62. Mohamed M *et al*. 2010 Epidemiologic and clinical aspects of a Rift Valley fever outbreak in humans in Tanzania, 2007. *Am. J. Trop. Med. Hyg*. **83**, 22–27. (doi:10.4269/ajtmh.2010.09-0318)
63. Hassan A *et al*. 2020 Epidemiological investigation of a Rift Valley fever outbreak in humans and livestock in Kenya, 2018. *Am. J. Trop. Med. Hyg*. **103**, 1649–1655. (doi:10.4269/ajtmh.20-0387)
64. Rugarabamu S, Mwanyika GO, Rumisha SF, Sindato C, Lim HY, Misinzo G, Mboera LEG. 2021 Seroprevalence and associated risk factors of selected zoonotic viral hemorrhagic fevers in Tanzania. *Int. J. Infect. Dis*. **109**, 174–181. (doi:10.1016/j.ijid.2021.07.006)
65. Rugarabamu S, Rumisha SF, Mwanyika GO, Sindato C, Lim HY, Misinzo G, Mboera LEG. 2022 Viral haemorrhagic fevers and malaria co-infections among febrile patients seeking health care in Tanzania. *Infect. Dis. Poverty* **11**, 33. (doi:10.1186/s40249-022-00959-z)
66. Madut DB *et al*. 2025 Epidemiologic and genomic characterization of an outbreak of Rift Valley fever among humans and dairy cattle in northern Tanzania. *J. Infect. Dis*. **232**, 298–307. (doi:10.1093/infdis/jiae562)
67. Shoemaker TR *et al*. 2018 Impact of enhanced viral haemorrhagic fever surveillance on outbreak detection and response in Uganda. *Lancet Infect. Dis*. **18**, 373–375. (doi:10.1016/s1473-3099(18)30164-6)
68. Gharpure R *et al*. 2025 Meeting report: CEPI workshop on Rift Valley fever epidemiology and modeling to inform human vaccine development, Nairobi, 4–5 June 2024. *Vaccine* **54**, 126860. (doi:10.1016/j.vaccine.2025.126860)
69. Eskew EA, Clancey E, Singh D, Situma S, Nyakarahuka L, Njenga MK, Nuismer SL. 2026 Supplementary material from: Interepidemic Rift Valley fever in East Africa: the recent risk landscape and projected impacts of global change. Figshare. (doi:10.6084/m9.figshare.c.8230314)